Evaluation of Rubber - Composites Bonding Components by Using Laser Electronic Shearography

Songping LIU, Feifei LIU, Legand LI, Enming GUO and Zhenghua CAO
The Center of NDT&E, Beijing Aeronautical Manufacturing Technology Research Institute; Beijing 100024, China
Phone: +86 10 85701657, Fax: +86 10 85702117; e-mail: liusping@publicb.bta.net.cn

Abstract

Laser electronic shearography is a fast, remote and global nondestructive testing and evaluation (NDT&E) method. The theoretic estimation results show that its sensitivity is dependent on surface deformation change $\Delta\delta_i^{1,2}$ of the object to be tested. Interferometric intensity coefficient $\Psi(\Delta\delta_i^{1,2})$ will change dramatically when $\Delta\delta_i^{1,2}$ is up to 0.1λ. Experimental and practical testing results have demonstrated that disbonding with Φ10 mm and voids with Φ3 – Φ5 mm in rubber-composite adhesive bonding interface can be found clearly and reliably by the method. A series of results – including 2D, 3D images, have been presented in this paper.

Keywords: Shearography, Nondestructive evaluation, Rubber-Composite bonding

1. Introduction

Rubber adhesive bonding structures have been applied increasingly in aviation, aerospace, machine and chemical industrial areas because of their unique properties – including sound absorption, damping, airproof, insulation, thermal barrier, etc. Rubber-composite bonding structures are the important new ones of rubber-nonmetal adhesive structures. They are rather sensitive to deviation of manufacturing technology parameters and tiny change(s) of environmental condition(s) during bonding process partly owing to the remarkable different physical and chemical properties of rubber and composite materials. Therefore, non-destructive testing and evaluation (NDT&E) are become a focal problem for rubber bonding structures in industrial applications.

Some literatures have paid their attentions on the NDT&E of rubber-metal bonding structures [1-3]. But with increasing applications of rubber–composite bonding structures in aviation and aerospace industrial areas their NDT&E has become more and more important. Firstly, quality, reliability and lifetime are the top concerning factors for aviation and aerospace applications. Secondly, rubber-composite bonding structures in aviation and aerospace are complex in shape and structure. We may not issue a NDT procedure by using conventional methods because of structural limitation, which results in a bad detectability. Another problem in NDT&E for these components is from material limitation. Sound absorption or attenuation is dramatically strong in rubber and NDT procedure can not be executed from composite base side of the bonding components.

Electronic speckle pattern interferometry (ESPI) non-destructive inspection is a possible and effective method for rubber-composite structures [4]. No special requirement of non-vibration environment is needed in ESPI method. Thus, it has been increasingly used to material characterization, interferometry measurement, materials and components NDT&E in Lab and in field [4-6]. Currently, with the development of ESPI NDT technique the testing results by the method can be visualized in 2- and 3-dimentional grey and/or color images

besides interferomery fringe pattern. It is called sherography[4] [6]. So far, shearography has been widely applied in NDT&E for composite materials structures, adhesive bonding components [3-6]. In this paper the investigation of NDT&E for rubber-composite bonding structures by using shearograpgy is introduced.

2. Rubber-composite bonding structure and testing method

Figure 1 gives the illustration of rubber-composite adhesive bonding structure. Rubber layer is bonded to the composite basic component. The testing is limit to rubber side because of limitation of the structures. Micro-deformation will take place in the rubber surface when a reasonable small loading is acted in the rubber. We may use δ_g to stand for the micro-deformation in the surface of rubber-composite bonding structure without defect in their bonding interface. When a disbonding is induced in the bonding interface, an additional deformation δ_d will be caused because of change of bonding interface integrality, which results in damage of loading transfer route in the structure body. The direction of deformation is dependence on the exerted loading. When the rubber surface is in pressured status under loading, a minus deformation $-\delta_d$ will occur in the surface of rubber-composites with disbanding. But a plus deformation $+\delta_d$ will come forth in the surface of rubber-composites with defect when the rubber surface is in pulled status under loading (see Fig. 1). The deformation can be recorded by using interferometry receiver and imaging system when a probe laser coherent beam is illuminated on the rubber surface. The coherent intensity ΣI_i received by the interferometry receiver in image plane can be expressed approximately by

$$\Sigma I_i = \Sigma[I_{1i} + I_{2i} + 2\sqrt{I_{1i} I_{2i}} \cos(2\pi\Delta\delta_{\mathrm{i}}^{1\,2} / \lambda)] \qquad (1)$$

where I_i is intensity corresponding to i^{th} rubber surface position, λ is the wavelength of probe laser, I_{1i} and I_{2i} are the intensity of i^{th} rubber surface position before and after deformation or neighbor deformation status during loading, respectively.

$\Delta\delta_{\mathrm{i}}^{1\,2}$ stands for the deformation change of rubber surface position i^{th} before and after loading. So, the coherent intensity in imaging plane is modulated by $\Delta\delta_{\mathrm{i}}^{1\,2}$.

(1) If no defect in rubber-composite bonding interface, then, $\Delta\delta_{\mathrm{i}}^{1\,2} = \delta_{\mathrm{gi}}^{1} - \delta_{\mathrm{gi}}^{2} = \Delta\delta_{\mathrm{gi}}^{1\,2}$. In this case, $\Delta\delta_{\mathrm{i}}^{1\,2}$ or $\Delta\delta_{\mathrm{gi}}^{1\,2}$ is determined by mechanical and physical properties of rubber-composite bonding structure at given conditions;

(2) When a disbonding defect exists in rubber-composite bonding interface, an additional deformation change $\Delta\delta_{\mathrm{di}}^{1\,2}$ will be caused by the disbonding: $\Delta\delta_{\mathrm{di}}^{1\,2} = \delta_{\mathrm{di}}^{1} - \delta_{\mathrm{di}}^{2}$. Then, $\Delta\delta_{\mathrm{i}}^{1\,2} = \Delta\delta_{\mathrm{gi}}^{1\,2} + \Delta\delta_{\mathrm{di}}^{1\,2}$. That's means that the deformation change of rubber surface position i^{th} is related to both mechanical and physical properties of rubber-composite bonding structure and defect. Usually, $\Delta\delta_{\mathrm{di}}^{1\,2} >> \Delta\delta_{\mathrm{gi}}^{1\,2}$. The deformation change can be recorded by using interferometry receiver. We also can get fringe pattern or image of measurements by means of signal processing and imaging techniques. It provides a remote, global and fast non-destructive inspection method for rubber-composite structures.

In case of $I_{1i} \approx I_{2i} \approx I_{0i}$, $\Sigma\Psi_{\mathrm{i}} = \Sigma \dfrac{I_i}{I_{0i}}$ is used to stand for intensity variation coefficient,

Then expression (1) can be rewrote as：

$$\Psi_i = 2\left[1+\cos\left(2\pi\Delta\delta_i^{1,2}/\lambda\right)\right], \qquad (2)$$

where Ψ_i is intensity change coefficient of rubber surface position i^{th} in imaging plane. It maps the intensity change at the i^{th} rubber surface position under loading.

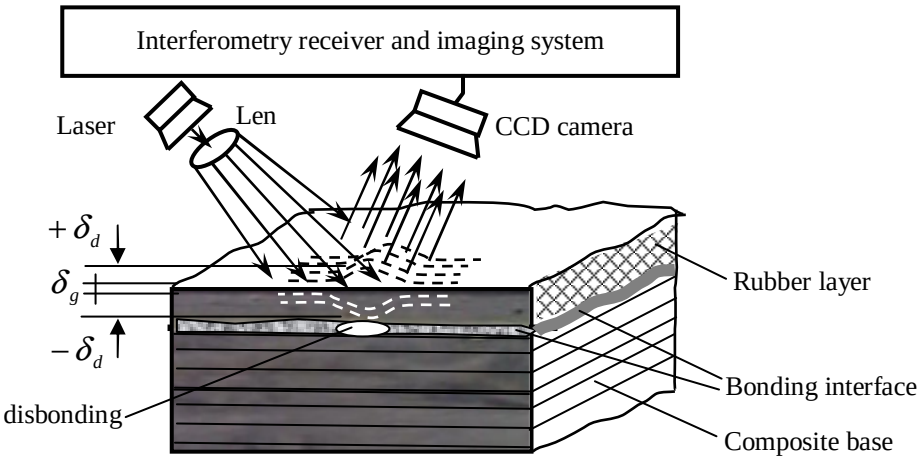

Figure 1. Illustration of the rubber-composite bonging structure and testing principle

$\Delta\delta_i^{1,2}$ is related to the size of load σ exerted at rubber surface position i^{th}. In order to estimate the affection of σ, i.e. $\Delta\delta_i^{1,2}$, on Ψ_i, $\Psi_i^{\sigma_0}(\Delta\delta_i^{1,2})$、$\Psi_i^{\sigma_1}(\Delta\delta_i^{1,2})$、$\Psi_i^{\sigma_2}(\Delta\delta_i^{1,2})$、$\Psi_i^{\sigma_3}(\Delta\delta_i^{1,2})$ and $\Psi_i^{\sigma_4}(\Delta\delta_i^{1,2})$ are used to stand for the coherent intensity change coefficient of i^{th} rubber surface position before and after loading when serials of different load σ_0, σ_1, σ_2, σ_3 and σ_4 are exerted at the i^{th} rubber surface position, separately. Then, $[(\Delta\delta_i^{1,2})^{\sigma_0}+0.01\lambda]$、$[(\Delta\delta_i^{1,2})^{\sigma_0}+0.05\lambda]$、$[(\Delta\delta_i^{1,2})^{\sigma_0}+0.1\lambda]$ and $[(\Delta\delta_i^{1,2})^{\sigma_0}+0.2\lambda]$ are supposed to be the deformation change at the i^{th} rubber surface position before and after the loadings. The estimation of $\Psi_i^{\sigma_0}(\Delta\delta_i^{1,2})$、$\Psi_i^{\sigma_1}(\Delta\delta_i^{1,2})$、$\Psi_i^{\sigma_2}(\Delta\delta_i^{1,2})$、$\Psi_i^{\sigma_3}(\Delta\delta_i^{1,2})$ and $\Psi_i^{\sigma_4}(\Delta\delta_i^{1,2})$ varied with deformation change are given in figure 2.

The theoretical estimation in figure 2 shows that: (1) the Ψ_i varies periodically with the deformation change $\Delta\delta_i^{1,2}$; (2) Variation of Ψ_i (i. e., I_i) is related to magnitude and distribution of $\Delta\delta_i^{1,2}$. No distinct change of Ψ_i will happen when $\Delta\delta_i^{1,2}$ is much smaller than laser wavelength. For example, $\Psi_i^{\sigma_1}$ is closed to $\Psi_i^{\sigma_0}$ in distribution because their deformation change difference (0.01λ) is very small (see Fig. 2). In that case no distinct fringe pattern or intensity change in distribution will occur. However, a remarkable variation of fringe pattern will be seen when deformation change is up to 0.05λ (see $\Psi_i^{\sigma_2}$、$\Psi_i^{\sigma_3}$、$\Psi_i^{\sigma_4}$ in Fig. 2). When deformation change of two neighbor coherent records is integral times of 0.5λ or 1λ during loading, the distribution in intensity is also no change. (3) Even a 0.0532μm deformation change will cause a significant Ψ_i change in distribution for wavelength 532nm coherent laser illuminator. For example, when $\Delta\delta_i^{1,2}$ changes from 0.3λ (approximately 0.16μm) to 0.4λ (approximately 0.21μm), Ψ_i

will change from 1.382 to 0.382, that means a distinct intensity change in distribution. Therefore, the sensitivity is very high and is related to the surface deformation change between two neighbor coherent records during loading.

In practical application a Mi*chelson* interferomtry is used to record surface deformation of rubber-composite bonding structures. Multiple images –including fringe pattern number distribution, 2D and 3D images, are reconstructed from measurements, so also called electronic shearographic imaging (ESI) method [7, 8].

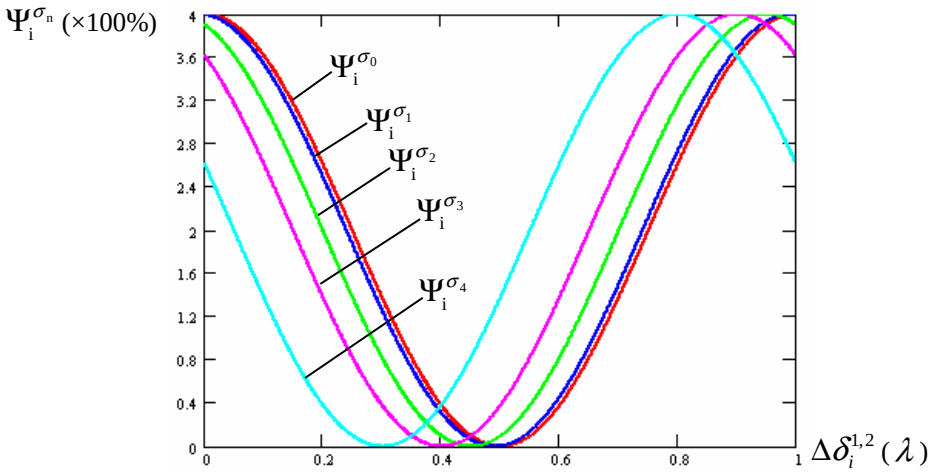

Figure 2. The estimation of ICC under different loadings

3. Experimental set-up

The scheme of employed experimental set-up consists of Mi*chelson* interferomrty unit, frame image record unit, computer system and laser illuminator. Results from measurements are organized in multiple forms –including fringe pattern, 2D and 3D images. A thermal loading is used in experiments. A 532 nm laser is used as illuminator.

A special specimen is designed to calibrate inspection sensitivity of the experimental set-up. The specimen is manufactured by using the same materials and composite structure units with a real rubber-composite component. The thickness of rubber is approximately 1mm. There are two metal bolts with Φ10mm and Φ13mm in composite base. Their surfaces of the bolts are located in the bonding interface. These two metal bolts provide a natural defect for testing calibration because of different thermal transmittivity between metal and composites.

4. Results and analysis

Figure 3 is the testing result from a real rubber-composite bonding component. The two defects with 13 mm and 10mm in diameters respectively are seen well according to the contrast distributions in figure 3 2D imaging results, as the areas marked by the white arrowheads. In defect zone the bonding interface is rubber-metal and other area is rubber-composite bonding interface. The deformation in rubber surface is different under thermal loading because of the evident distinctness in heat conduction between metal and composites substrates. Thus, the deformation change $\Delta\delta$ on the surfaces of rubber-composites bonding zone and rubber-metal bonding zone is obviously different. This difference in $\Delta\delta$ gives a remarkable change between $\Psi(\delta+\Delta\delta)$and $\Psi(\delta)$ (see Fig. 2). Therefore, the significantly different contrast distribution can be visualized in defect zones in figure 3 compared with that in good areas.

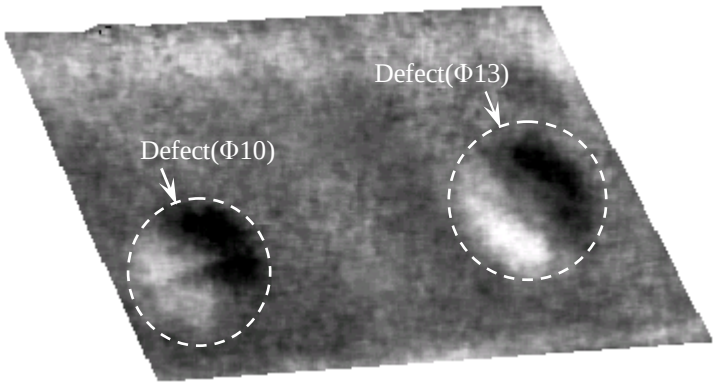

Figure 3. 2D imaging in the area with simulated defects

A real testing result from a practical rubber-composite bonding component is given in figure 4. The tested area is about 340(x)×70(y)mm. Figure 4(a) is the 2D imaging result. Figure 4(b) is the fringe pattern number (FPN) distribution corresponding to the position marked by the white dashed line in figure 4(a). The contrast distribution in 2D image shows clearly the existence of many voids in rubber-composite bonding interface, as the zones showed by the white arrowheads. The existence of the voids can be visualized more clearly according to the FPN distribution in figure 4(b). An obvious FPN peak occur in void, as showed in figure 4(b). This is because the deformation change $\Delta\delta_d$ in void zone is much bigger than $\Delta\delta_g$ in good zone. Thus, the difference of $\Psi(\delta_d+\Delta\delta_d)$ and $\Psi(\delta_d)$ is significant in void zone, but in good zone the difference of $\Psi(\delta_g+\Delta\delta_g)$ and $\Psi(\delta_g)$ is tiny.

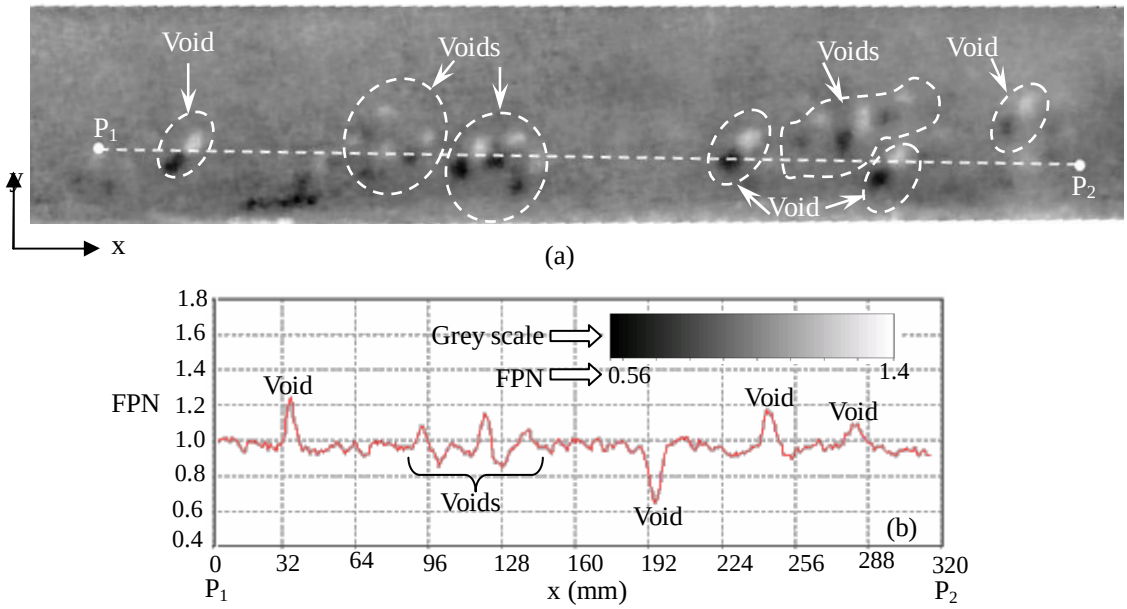

Figure 4. The shearogragphic imaging results from a practical rubber-composite bonding component. (a) 2D image, (b) FPN distribution corresponding to the marked position by the white line P_1-P_2 in (a)

A visualized view of these voids –including their positions and distributions, can be

found by using 3D imaging in figure 5. Their sizes are found to be in the order of 3-5mm in diameter after a destructive testing. The possible reason caused these voids are resulted from adhesive bonding processing.

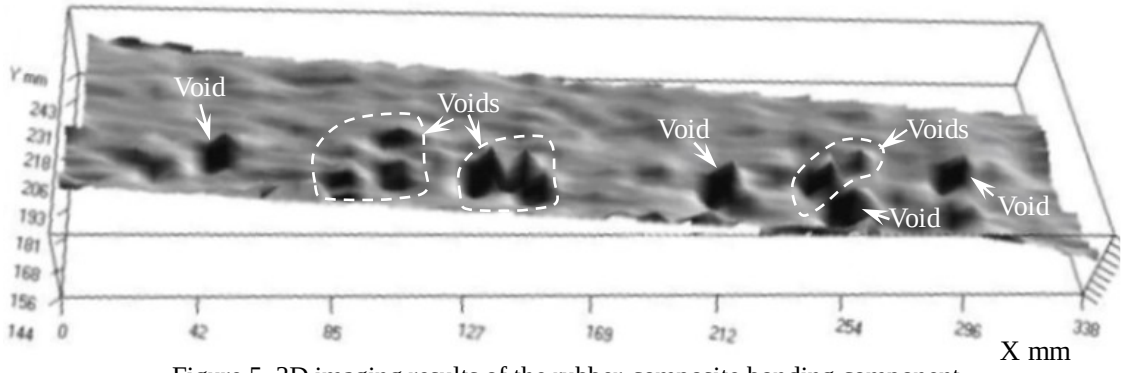

Figure 5. 3D imaging results of the rubber-composite bonding component

4. Conclusion

(1) The theoretic estimated results show that sensitivity of ESI is related to deformation change $\Delta\delta$ at surface of rubber-composite components to be tested. A measurable surface micro-deformation change $\Delta\delta$ will cause a remarkable $\Psi(\delta+\Delta\delta)$ change under reasonable loading. The $\Delta\delta$ is closed to 0.532μm for 532nm laser luminaire, therefore, the sensitivity of this method is very high.

(2) Multiple images –including fringe pattern, 2D, 3D images, can be reconstructed by using measured data of ESI.

(3) The experimental and practical results show that the ESI method provides an effective NDT&E of rubber-composite bonding structures. Voids with 3-5 mm in diameter in rubber-composite bonding interface can be reliably found out by using this method.

References

[1] Matzkanin, G., Nondestructive evaluation of rubber/metal adhesive bonds using oblique incidence ultrasonics, NDE of Adhesive Bonds and Bondlines, Topical Proceedings [M], Valley Forge. Pennsylvannia (United States), ASNT (1989), 9-13 Oct. 1989, pp60-61.

[2] A. C. Smith and H. Yang, Ultrasonic Study of Adhesive Bond Quality at a Steel-to-Rubber Interface by Using Quadrature Phase Detection Techniques, Materials Evaluation[J], 1989, 47./December, pp1398-1400.

[3] Songping Liu, Enming Guo, et al, Resaerch on the evaluation of the steel-rubber adhesive bonding of solid propeller cover by ultrasonic reflection technique , Nondestructive testing [J], Vol. 25, No. 10 (2003), pp495-499.

[4] Hung, Y. Y., Shearography: A New Optical Method for Strain Measurement and Nondestructive Testing, Optical Engineering [J], Vol .21, 1982, pp391-395.

[5] Lockberg, D. J, J. T. Malmo and G.A. Slettemden, Interferometric Measurements on High temperature objects by Electronic Speckle Pattern Interferometry, applied Optics[J], Vol.24, 1985, pp3167-3172.

[6] R Gregory, Composite repair inspection by laser Shearography, Insight [J], Vol.45, No.3, 2003, pp183-185.

[7] James B. Spicer, John L. Champion, Robert Osiander and Jane W. M. Spicer, Time resolved shearographic and thermographic NDE methods for graphite epoxy/honeycomb composite [J], Materials Evaluation, October, 1996, pp1210-1213.

[8] Songping Liu, Zhenghua Cao, et al, Advanced electronic shearography imaging

technique，8th NDT Cconference, Su Zhou, China, 22-25 September, 2003.